www.czasopisma.pan.pl PAN POLSKA AKADEMIA NAUK www.journals.pan.pl

A R C H I V E S O F M E T A L L U R G Y A N D M A T E R I A L S

Volume 58 2013 Issue 3

DOI: 10.2478/amm-2013-0058

M. MADEJ*

PHASE REACTIONS DURING SINTERING OF M3/2 BASED COMPOSITES WITH WC ADDITIONS

ANALIZA SPIEKANIA KOMPOZYTÓW STAL SZYBKOTNĄCA M3/2 – WĘGLIK WOLFRAMU WC

Attempts have been made to describe the influence of WC additions on properties of M3/2 high speed steel (HSS) based composites. The powder compositions used to produce skeletons for further infiltration were M3/2, M3/2+10%WC and M3/2+30%WC. The powders were cold pressed at 800 MPa. The green compacts were subsequently sintered for 60 minutes at 1150°C in vacuum. These as-sintered specimens were used for copper infiltration. A qualitative EDX analysis revealed presence of both MC type vanadium-rich carbides and M_6C type tungsten and iron rich carbides. In specimens containing 10 and 30% WC the carbide phase was uniformly distributed within copper-rich regions. The WC monocarbide reacts with the surrounding HSS matrix and forms a carbide grain boundary film. The microstructural observations of the as-sintered specimens was followed by Brinell hardness test and supplemented with dilatometric studies.

Keywords: M3/2 High speed steel (HSS), tungsten carbide WC, copper, metal matrix composites (MMC), sintering, infiltration

Badania miały na celu określenie wpływu dodatku węglika wolframu WC na własności kompozytów na osnowie stali szybkotnącej. Do wytwarzania porowatych kształtek stosowano następujące mieszanki proszków: 100% M3/2, M3/2+10%WC i M3/2+30%WC. Mieszanki proszków prasowano pod ciśnieniem 800MPa. Część wyprasek poddano spiekaniu przez 60 minut w temperaturze 1150°C w próżni lepszej od 10^{-2}. Do infiltracji stosowano wypraski i porowate spieki. Analiza przy użyciu mikrosondy rentgenowskiej potwierdziła obecność dwu typów węglików: MC bogatych w wanad oraz M_6C bogatych w wolfram i żelazo. W kształtkach z dodatkiem 10 i 30% węglika wolframu następuje rozpuszczanie węglika i rekcja z osnową stali szybkotnącej, w wyniku czego powstaje nowy węglik w postaci filmu otaczającego cząstki dodanego węglika wolframu. Dodatkowo przedstawiono wyniki badań twardości, wytrzymałości na zginanie oraz odporności na zużycie ścierne badanych kompozytów.

1. Introduction

Design criteria for high strength tool materials are: high hardness, good wear resistance and adequate toughness. Cold compaction and vacuum sintering of PM high speed steels to full density is now a well established technique [1-3]. In recent years, extensive work has been undertaken to sinter metal matrix composites (MMCs) which contain ceramic particles embedded in a HSS matrix. Most studies have been focused on sintered HSSs with additions of hard ceramics such as Al_20_3, VC, NbC, TiC, WC and TiN with the aim of producing a more wear resistant HSS-base material [4-18]. These composites have been developed for harsh wear applications as an attractive alternative to expensive cemented carbides. They have higher hardness, elastic modulus and resistance to wear than high strength steels, however, the addition of brittle ceramic particles may degrade toughness as the reinforcing particles promote crack initiation. In order to ensure good bonding at the ceramic/matrix interfaces, the ceramic particles must exhibit some reactivity with the matrix. Except for Al_2O_3, which does not react with the HSS matrix, diffusion of iron into the MC carbide particles give rise to good cohesion across the ceramic/matrix interface. Besides, MC carbides are relatively stable in contact with iron during sintering and do not dissolve extensively. Therefore, MC particles were chosen as the reinforcement.

An inexpensive and easy route to develop HSSs reinforced with MC carbides consists of mixing commercial HSS powders with carbides. High hardness, mechanical strength, heat resistance and wear resistance of HSSs make them an attractive material for manufacture of MMCs. HSSs comprise a family of alloys mainly used for cutting tools. Their name – high speed steel – is a synthesis of the following two features [11]:

1. the alloys belong to the Fe-C-X multicomponent system, where X represents a group of alloying elements in which Cr, W, Mo, V and Co are the principal ones;
2. the alloys are characterized by their capacity to retain high hardness when exposed to elevated temperatures resulting from cutting metals at high speeds.

The carbides are mainly formed by strong carbide formers, i.e. V, W, Mo and Cr. Depending on the alloy composition

* AGH UNIVERSITY OF SCIENCE AND TECHNOLOGY, FACULTY OF METAL ENGINEERING AND INDUSTRIAL COMPUTER SCIENCE, AL. A. MICKIEWICZA 30, 30-059 KRAKÓW, POLAND

and its thermal processing parameters (sintering temperature and cooling rate) various types of carbides, such as M_6C, M_2C, MC and $M_{23}C_6$, can be formed. The carbides can grow directly from the melt during solidification or they are created by eutectic reaction or by decomposition of other types of carbide. The latter case is well exemplified by the decomposition of M_2C carbide into M_6C and MC when annealing HSSs in excess of 1000°C. The alloying elements affect the type of carbide, its formation temperature and crystal structure. MC, M_6C and $M_{23}C_6$ carbides have a fcc structure, whereas the metastable M_2C has a hcp structure. The carbides are also different in composition with higher V and Ti, and lower Fe and Cr levels in MC as compared with M_6C and M_2C, which are rich in Mo and W. $M_{23}C_6$ carbide, contained in annealed HSSs, is rich in Cr, with high content of Fe, which substitutes Cr, and low contents of W and Mo.

Considering the M3/2 grade of HSS it is evident that the formation of M_6C grain boundary film is the key problem in sintering to full density. The alloy composition favours formation of a certain type of carbide. For a given amount of V, increased W concentrations favour formation of M_6C at the expense of MC, whereas Mo has the opposite effect. The volume fraction of eutectic carbides increases in proportion to the carbon content. Many studies demonstrate how the as-sintered microstructure can be tailored by adding elemental powders to a gas atomised M3/2 HSS powder. Applications of elemental Si to repel C from the melt during sintering, elemental Ni to stabilize austenite, and elemental V to form MC at the expense of cementite are well documented [15÷21]. Additions of carbides to HSSs have also been studied [9-19]. Thermodynamically less stable carbides, such as SiC and Cr_3C_2, easily dissolve in the matrix during sintering or annealing. Intermediate carbides, such as WC, VC, Mo_2C and NbC, react with the matrix to produce other carbide phases with compositions similar to primary carbides, e.g M_6C (Fe_3W_3C or Fe_3Mo_3C) and niobium or vanadium rich MC type carbides. Thermodynamically stable carbides such as TiC are retained in their original form but also encourage formation of MC carbides at the TiC/matrix interface. Generally TiC additions decrease sinterability by raising the sintering temperature required to achieve a pore-free material. It has been reported that additions of TiC decrease bending strength of HSSs and cause negligible increase in hardness [18,19].

2. Experimental procedure

Water atomised M3/2 grade powder, finer than 160μm, was delivered by POWDREX SA in as-annealed condition. Its microstructure consists of fine carbides embedded in a martensitic/bainitic matrix and particle microhardness $HV_{0,065}$ = 284 ±17 [5].

The chemical composition of the M3/2 grade powder is given in Table 1.

TABLE 1

Chemical composition of the experimental M3/2 HSS powder, wt-%

C	Cr	Co	Mn	Mo	Ni	Si	V	W	Fe	O
1,23	4,27	0,39	0,21	5,12	0,32	0,18	3,1	6,22	balance	0,0626

Commercial tungsten carbide, having a mean particle size of 3 μm, was used as an additive. The particle shape of the experimental powders is shown in Fig. 1.

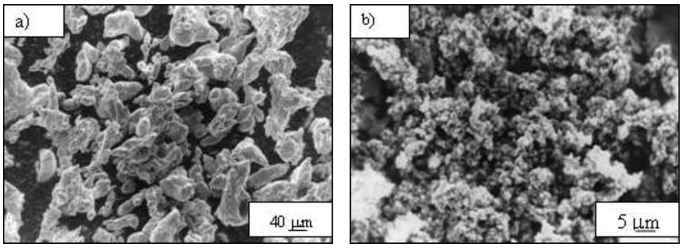

Fig. 1. SEM micrographs of: a) water atomized HSS M3/2 powder, b) fine WC powder

The experimental powders were used to prepare three composite materials. Their powder compositions are presented in Table 2.

TABLE 2

Powder compositions of the experimental composites

Material designation	Powder composition, wt-%	
	M3/2	WC
M	100	0
M10WC	90	10
M30WC	70	30

The powders were mixed in a Turbula type mixer for 30 minutes and cold pressed in a rigid cylindrical die at 800 MPa. Green compacts were subsequently sintered for 60 minutes at 1150°C in vacuum better than 10^{-2} Pa. The sintering process was concurrently studied by means of dilatometric measurements.

Both green and as-sintered densities of the porous bodies were measured prior to infiltration using the Archimedes method. The measured densities were divided by theoretical densities (ρ_t) to calculate relative densities. The theoretical densities for the composites were calculated using the following equation:

$$\rho_t = (\rho_a \cdot X_a + \rho_b \cdot X_b) \quad (1)$$

where ρ_a and X_a are density and volume fraction of WC; similarly ρ_b and X_b are density and volume fraction of M3/2 HSS.

Prior to infiltration the porous skeletons were also tested for Brinell hardness.

The infiltration process was carried out in vacuum better than 10^{-2} Pa. Both green compacts and preforms, sintered for 60 minutes at 1150°C in vacuum, were infiltrated with copper. Carefully pre-weighed pieces of copper infiltrant were placed on top of the rigid skeletons of predetermined porosity, heated to 1150°C, held at temperature for 15 minutes, and cooled down with furnace to room temperature.

After infiltration the composites were examined microscopically by means of the light microscopy (LM) and scanning electron microscopy (SEM). The phase composition was examined by both the energy-dispersive X-ray spectroscopy (EDX) and X-ray diffraction (XRD).

3. Results and discussion

The combined effects of WC content and powder processing route on relative density, shrinkage and Brinell hardness of porous skeletons are shown in Figures 2, 3 and 4.

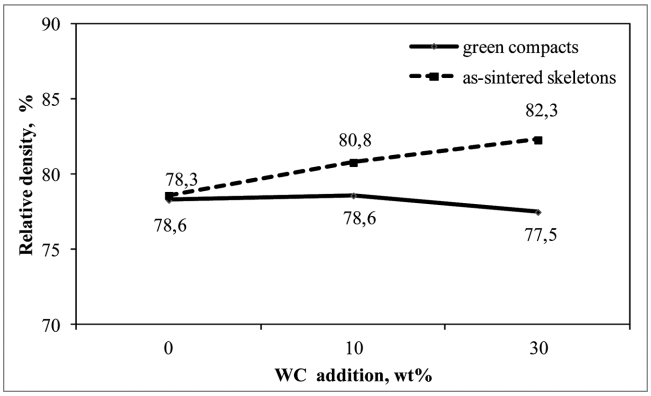

Fig. 2. Relative density of green compacts and sintered porous skeletons as a function of WC addition

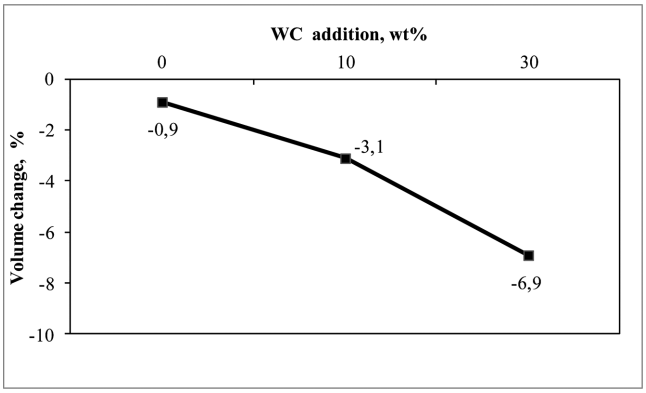

Fig. 3. Volume changes of compacts during sintering as a function of WC addition

Figures 2 and 3 show the effect of WC content on compressibility and volume changes during sintering of the M3/2 HSS skeletons. The green density of compacts slightly decreases with increasing WC content, whereas additions of tungsten carbide, up to 30%, increase the as-sintered density and Brinell hardness of the HSS-base composites (Figure 4).

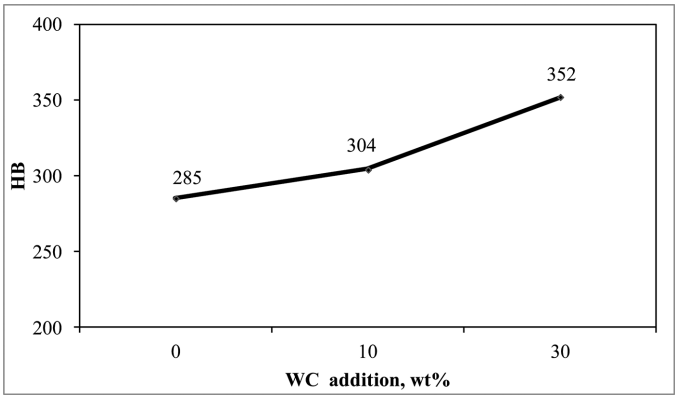

Fig. 4. Brinell hardness of sintered porous skeletons as a function of WC addition

Figure 5 shows that the M3/2 grade HSS cannot be fully densified at 1150°C, and that the as-sintered density is approximately equal to the green density. Additions of 30% tungsten carbide increase the as-sintered density presumably due to the occurrence of a liquid phase due to dissolution of tungsten carbide particles in the matrix. As exemplified in Figure 5, marked specimen expansion followed by its rapid contraction has indicated that the liquid appears between 1080 and 1110°C. Intermediate carbides, such as WC, partially dissolve and react with the steel constituents to produce a new carbide phase with a composition similar to primary carbides present in HSSs.

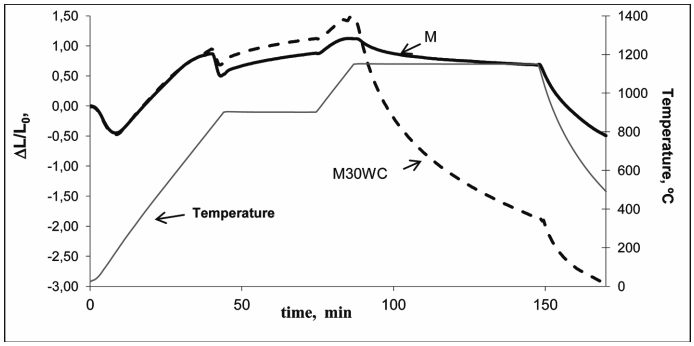

Fig. 5. Dilatometric curves recorded for the M3 and M30WC skeletons

4. Phase analysis

Phase identification of the composites was performed using a Tur 62 X-ray diffractometer and Cu K_α radiation (λ = 1.5406Å).

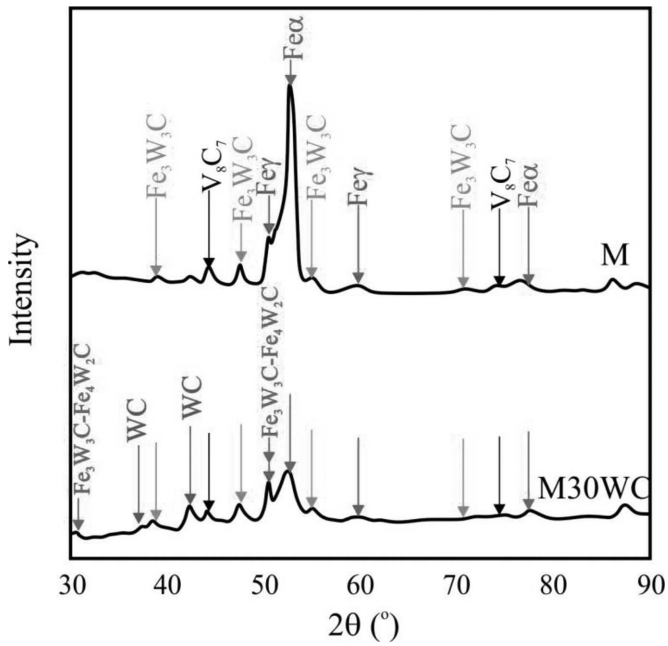

Fig. 6. XRD patterns recorded for as-sintered M and M30WC skeletons

From the XRD patterns in Figure 6 it is evident that M_6C (Fe_3W_3C) and MC (V_8C_7) carbides, ferrite and austenite are present in the as-sintered M sample, whereas M_6C (Fe_3W_3C and Fe_3W_3C-Fe_4W_2C) and MC (WC and V_8C_7) carbides, ferrite and austenite have been found in the M30WC sample. As compared to the M material the intensity of Fe_α peaks in

pre-sintered M30WC samples is smaller at the expense of WC and Fe_3W_3C-Fe_4W_2C peaks.

The SEM-EDX analysis performed on specimens containing 10 and 30% WC have revealed the carbide phase evenly distributed within the steel matrix. From Figure 7 it is evident that during sintering of porous skeletons the added WC reacts with the HSS matrix to form iron-rich Fe_3W_3C-Fe_4W_2C carbides.

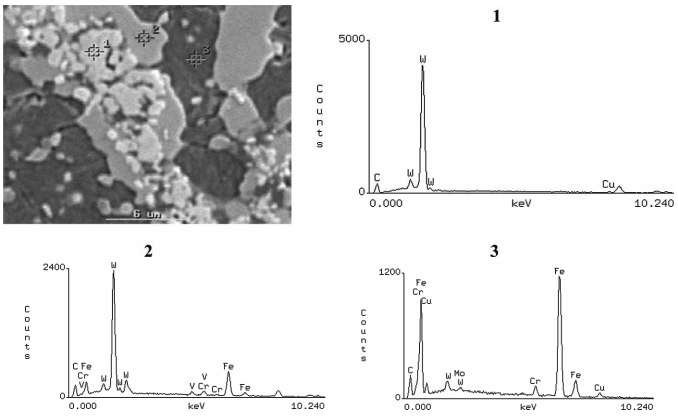

Fig. 7. Microstructure of the M30WC composite and EDX spectra

As shown in Figures 8÷10, the as-infiltrated properties of the investigated composites depend on their manufacturing route and WC additions.

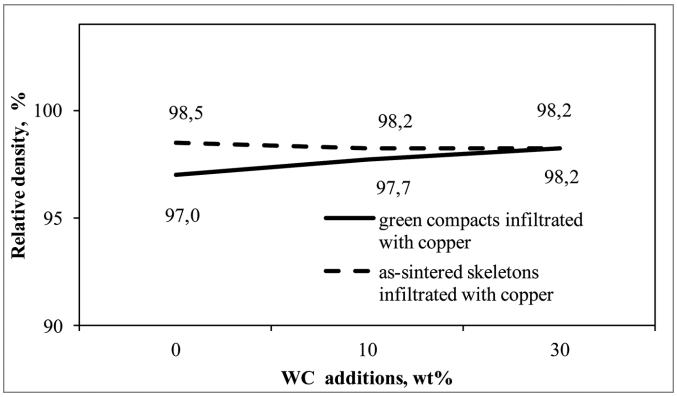

Fig. 8. Relative density of as-infiltrated composites

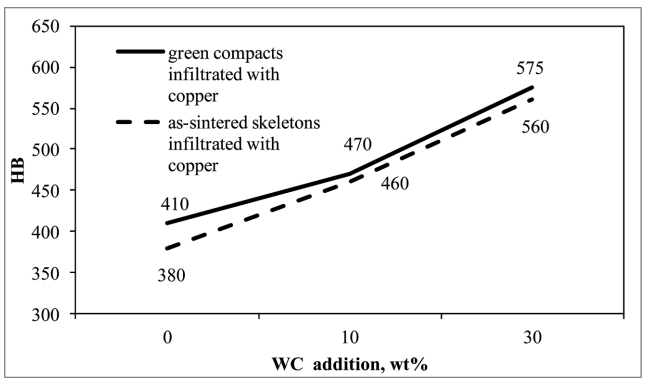

Fig. 9. Brinell Hardness of as-infiltrated composites

From Figure 8 it is evident that the molten copper is drawn into the interconnected pores of the skeleton, through a capillary action, and fills virtually the entire pore volume to yield the final density exceeding 97% of the theoretical value. Infiltration of as-sintered skeletons with copper results in slightly higher relative densities of M and M10WC composites due to reduction of oxides present at powder surface.

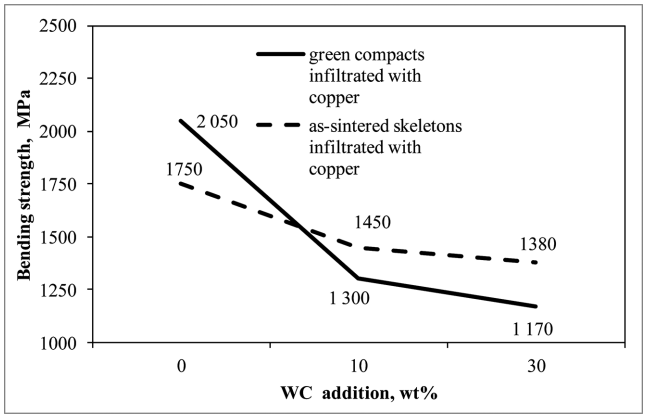

Fig. 10. Bending Strength of as-infiltrated composites

The Brinell hardness of the as-infiltrated composites increases with the WC addition. Slight difference in hardness between the materials obtained from the two manufacturing routes was observed, i.e. higher hardness was achieved after infiltration of green compacts. This can be explained by the reduction of carbon content taking place during pre-sintering. The Bending Strength of the as-infiltrated composites decreases with increasing the content of hard WC powder in the mix.

The wear tests were carried out using the block-on-ring tester (Figure 11).

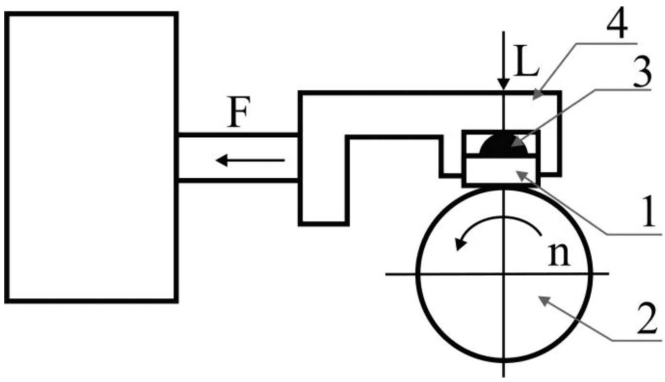

Fig. 11. Schematic view of a block-on-ring tester

During the test a rectangular 20×4×4 mm wear sample (1) was mounted in a sample holder (4) equipped with a hemispherical insert (3) ensuring proper contact between the test sample and a steel ring (2), heat treated to 55 HRC, which was rotated at a constant speed of 500 rpm. The wear surface of the sample was perpendicular to the loading direction. Double lever system was used to force the sample towards the ring at 165 N ±1%. The loss of sample mass was measured after a sliding distance of 1000 m.

Before testing for wear, all specimens were polished to an average roughness of R_a = 1 μm. The tests were carried out at room temperature, keeping a relative humidity below 30%. The loss of mass of the wear samples is given in Figures 12÷13.

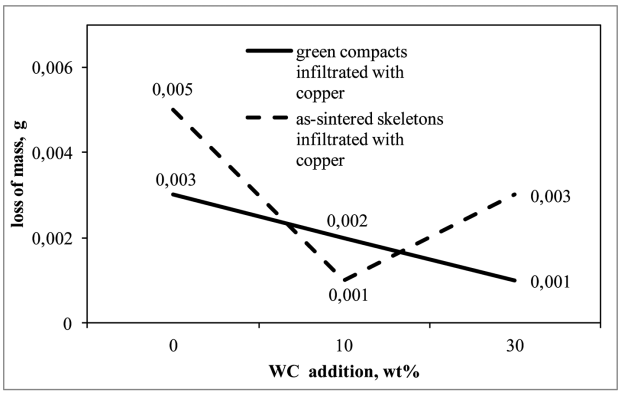

Fig. 12. Loss of mass of as infiltrated composites

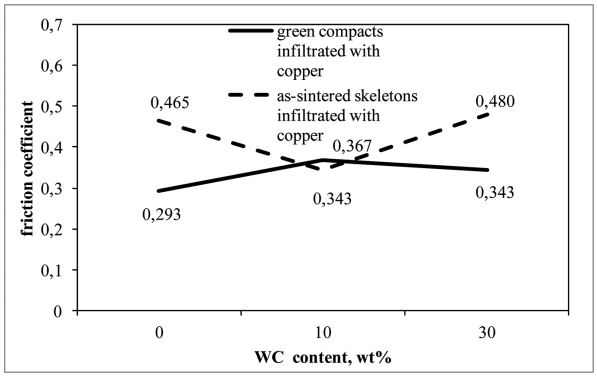

Fig. 13. Friction coefficient of as infiltrated composites

Generally direct infiltration of green compacts with copper results in higher wear resistance and lower friction coefficient. of the as-infiltrated M and M30WC composites, although the friction coefficients are not highly influenced by the WC additions and the obtained wear data seems to be markedly affected by the sample preparation and experimental conditions.

5. Microstructures

Typical microstructures of copper infiltrated green compacts and pre-sintered skeletons are shown in Figures 14-16.

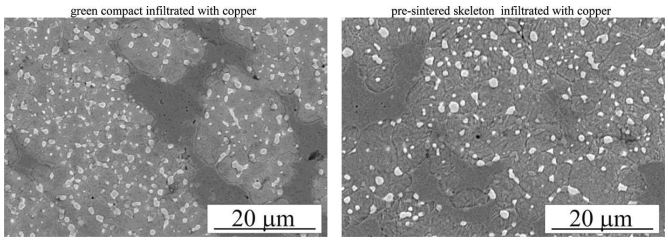

Fig. 14. Microstructures of M based composites, SEM

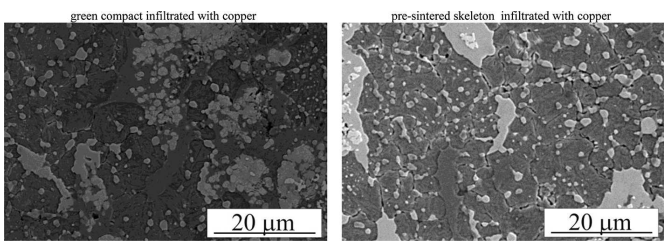

Fig. 15. Microstructures of M10WC based composites

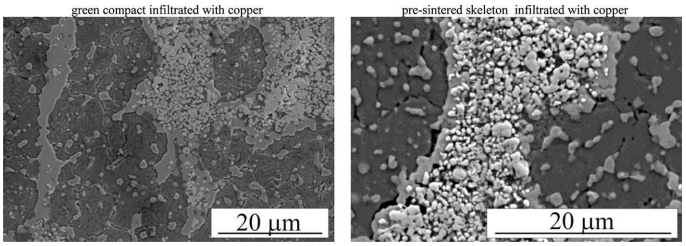

Fig. 16. Microstructures of M30WC based composites

Typical microstructures of as-sintered M3/2 baseline material are composed of a martensitic matrix, retained austenite, M_6C and MC type carbides [18,19] both located within the grains and forming a grain boundary film. As can be seen in Figures 14-16, the microstructure of the M3/2 based composites infiltrated with copper is similar except for the copper areas. Regardless of the infiltration route the tested composites have almost pore-free microstructure. The WC powder admixed to the M3/2 grade HSS markedly influenced the microstructure of the composites. Some WC particles were retained in the microstructure but a part of the tungstene monocarbide came into reaction with the M3/2 steel components to form vanadium and iron containing M_6C carbides (Figure 7). These M_6C had a tendency to form a continuous layer surrounding the added WC particles.

6. Conclusions

- Direct infiltration of green compacts with copper results in the higher hardness and wear resistance of composites and allows to cut the production cost.
- Typical microstructure of the M10WC and M30WC composites infiltrated with copper is composed of tempered martensite, residual austenite, copper regions, MC and M_6C carbides.
- The morphology and distribution of carbides depend on WC contents and production process parameters. Iron-rich M_6C type carbides (Fe_3W_3C-Fe_4W_2C) are formed during sintering as a result of chemical reaction between the added WC and matrix of the M3/2 steel.
- The mechanical properties of the tested composites strongly depend on the amount of WC added. The additions of WC increase hardness and decrease bending strength of the composites.
- The wear resistance of the tested composites is very high but the results are inconsistent and seem to be affected by the testing conditions.

Acknowledgements

This work was financed by Ministry of Science and Higher Education through the project No 11.11.110.788.

REFERENCES

[1] G. G r e e t h a m, Development and performance on infiltrated and non-infiltrated valve seat insert materials and their performance. Powder Metallurgy **3**, 2, 112-114 (1990).

[2] R.H. Plama, Tempering response of copper alloy-infiltrated T15 high-speed steel, The International Journal of Powder Metallurgy **37**, 5, 29-35 (2001).
[3] C.S. Wright, The production and application of PM high-speed steels. Powder Metallurgy **3**, 937-944 (1994).
[4] J.M. Torralba, G. Cambronero, J.M. Ruiz-Pietro, M. M das Neves, Sinterability study of PM M2 and T15 HSS reinforced with tungsten and titanium carbides **36**, 55-66 (1993).
[5] M. Madej, J. Leżański, Copper infiltrated high speed steel based composites, Archives of Metallurgy and Materials **50**, 4, 871-877 (2005).
[6] M. Madej, J. Leżański, The structure and properties of copper infiltrated HSS based, Archives of Metallurgy and Materials **53**, 3, 839-845 (2008).
[7] K. Żaba, The influence of temperature and time of exhibition on a change of Al-Si coating thickness and surface texture on the steel plates, Archives of Metallurgy and Materials **55** (1), 151-162 (2010).
[8] B. Leszczyńska-Madej, The effect of sintering temperature on microstructure and properties of Al – SiC composites Archives of Metallurgy and Materials **58**, 1 (2013).
[9] A. Głowacz, Z. Głowacz, Diagnostics of dc machine based on analysis of acoustic signals with application of mfcc and classifier based on words, Archives of Metallurgy and Materials **57**(1), 179-183 (2012).
[10] Farid Akhtar, Microstructure evolution and wear properties of in situ synthesized TiB2 and TiC reinforced steel matrix composites, Journal of Alloys and Compounds **459**, 491-497 (2008).
[11] G. Hoyle, High Speed Steels. Butterworth & Co. Publishers. Cambridge 1998.
[12] S. Wei, J. Zhu, L. Xu, Effects of vanadium and carbon on microstructures and abrasive wear resistance of high speed steel, Tribology International **39**, 641-648 (2006).
[13] Z. Zalisz, A. Watts, S.C. Mitchell, A.S. Wronski, Friction and wear of lubricated M3 Class 2 sintered high speed steelwith and without TiC and MnS additives, Wear **258**, 701-711 (2005).
[14] W.C. Zapata, C.E. Da Costa, J.M. Torralba, Wear and thermal behaviour of M2 high-speed steel reinforced with NbC composite, Journal of Materials science **33**, 3219-3225 (1998).
[15] G.A. Baglyuk, L.A. Poznyak, The sintering of powder metallurgy high-speed steel with activating additions, Powder Metallurgy and Metal Ceramics **41**, 7-8, 366-368 (2002).
[16] W. Khraisat, L. Nyborg, P. Sotkovszki, Effect of silicon, vanadium and nickel on microstructure of liquid phase sintered M3/2 grade high speed steel, Powder Metallurgy **48**, 1, 33-38 (2005).
[17] J.A. Jiménez, M. Carsı, G. Frommeyer, O.A. Ruano, Microstructural and mechanical characterisation of composite materials consisting of M3/2 high speed steel reinforced with niobium carbides, Powder Metallurgy **48**, 4, 371-376 (2005).
[18] J.D. Bolton, A.J. Gant, Phase reactions and chemical stability of ceramic carbide and solid lubricant particulate additions within sintered high speed steel matrix, Powder Metallurgy **36**, 4, 267-274 (1993).
[19] J.D. Bolton, A.J. Gant, Heat treatment response of sintered M3/2 high speed steel composites containing additions of manganese sulphide, niobium carbide, and titanium carbide, Powder Metallurgy **39**, 1, 27-34 (1996).
[20] M. Madej, Copper infiltrated high speed steel based composites with iron additions, Archives of Metallurgy and Materials **54**, 4, 1083-1091 (2009).
[21] M. Madej, The tribological properties of high speed steel based composites, Archives of Metallurgy and Materials **55**, 1, 61-68 (2010).
[22] H.G. Rutz, F.G. Hanejko, High density processing of high performance ferrous materials, international conference & Exhibition on powder Metallurgy & Particulate Materials, May 8-11, 1994 – Toronto, Canada.
[23] M.M. Oliveira, High-speed steels and high-speed steels based composites. International Journal of Materials and Product Technology **15**, 3-5, 231-251 (2000).

Received: 20 March 2012.